

Syntheses and structures of Li, Fe, and Mo derivatives of *N,N'*-bis(2,6-diisopropylphenyl)-*o*-phenylenediamine†Trevor Janes,<sup>a</sup> Jeremy M. Rawson<sup>b</sup> and Datong Song<sup>\*a</sup>

Cite this: DOI: 10.1039/c3dt51063h

Received 22nd April 2013,  
Accepted 20th May 2013

DOI: 10.1039/c3dt51063h

www.rsc.org/dalton

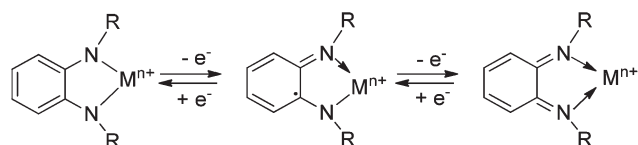
Double deprotonation of *N,N'*-bis(2,6-diisopropylphenyl)-*o*-phenylenediamine ( $H_2L$ ) with *n*-BuLi in THF yields the dilithium complex  $Li_2L(thf)_3$ . The reaction of  $Li_2L(thf)_3$  with  $FeBr_2(thf)_2$  and subsequent replacement of the solvent with toluene yield  $LFe(\eta^6\text{-toluene})$ , which can also be synthesized from  $Fe(HMDS)_2(thf)$  and  $H_2L$  in toluene. The NMR data, bond lengths obtained from an X-ray diffraction study, and DFT calculations indicate that the diamide ligand  $L^{2-}$  undergoes oxidation to a radical ligand  $L^{1\cdot-}$ . Reaction of  $LFe(\eta^6\text{-toluene})$  with 1 atm CO yields the tricarbonyl complex  $LFe(CO)_3$ .  $MoCl_4(thf)_2$  reacts with two equivalents of  $Li_2L(thf)_3$  to yield  $(LiL)_2MoCl_2(thf)_4$  in which the phenylene backbone of the ligand has been dearomatized. One-electron oxidation of  $Li_2L(thf)_3$  by  $EuCl_3(dme)_2$  yields the open-shell species  $LiL(OEt)_2$ , which was characterized by X-ray crystallography and EPR spectroscopy.

## Introduction

The study of redox-active ligands has led to clearer understanding of fundamental coordination chemistry<sup>1</sup> as well as exciting new examples of catalysis including the use of abundant first-row metals.<sup>2,3</sup> *o*-Phenylenediamine (pda) derivatives are classic examples of redox-active ligands. Scheme 1 depicts the three possible redox forms of this ligand series with *o*-phenylenediamide ( $pda^{2-}$ ) as its most reduced form, and *o*-diimino-semiquinonate ( $pda^{1\cdot-}$ ) and *o*-benzoquinonediimine ( $pda^0$ ) as intermediate and most oxidized forms, respectively. Early reports from Holm emerged in the 1960s on the synthesis and electrochemical behaviour of late-transition metal complexes of the various redox forms of pda.<sup>4,5</sup> To date the

unsubstituted,<sup>4–11</sup> *N*-monosubstituted,<sup>12–17</sup> and *N,N'*-disubstituted variants of this family of ligands have been synthesized and employed as ancillary ligands for main group<sup>18,19</sup> and transition metals.<sup>20–26</sup>

The 2,6-diisopropylphenyl (dipp) group has found use in chelating ligand design because it can provide unique sterics around the metal centre, which can stabilize coordinatively unsaturated metal centres. Despite the popularity of the dipp group in ligand design and the ease of preparation of the dipp-substituted pda,<sup>27</sup> the coordination chemistry of a dipp-substituted pda ligand is underexplored compared to other pda derivatives. Only recently the dipp-substituted  $pda^{2-}$  ligand has found use in the isolation of boryl anions.<sup>28</sup> Our group is interested in exploring the coordination chemistry of this ligand toward transition metals. Herein we report the synthesis and characterization of the dilithium salt of this ligand, its coordination behaviour towards Fe and Mo, as well as the synthesis and characterization of the monolithium salt of the corresponding dipp-substituted  $pda^{1\cdot-}$  ligand.



Scheme 1

## Results and discussion

## Synthesis of dilithium complex 2

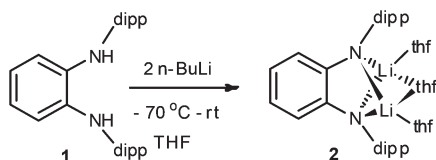
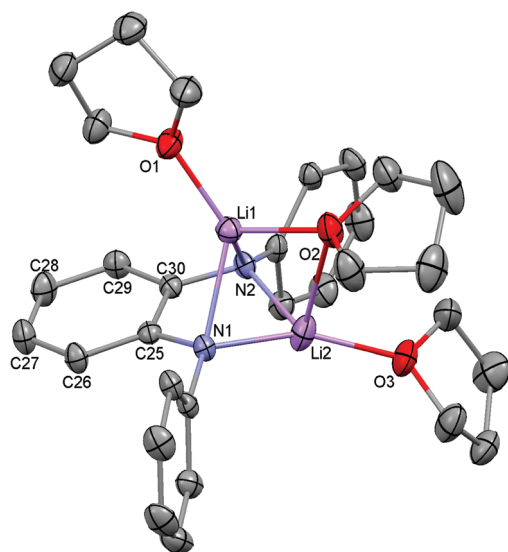
As shown in Scheme 2, diamine **1** can be doubly deprotonated at  $-70^\circ\text{C}$  with two equiv. of *n*-butyl lithium in THF and the dilithium complex **2** forms as a precipitate. The solid state structure of **2** has been confirmed by X-ray crystallography. As shown in Fig. 1, Li1 adopts a highly distorted tetrahedral coordination geometry with two amido nitrogen donor atoms, one oxygen donor atom from a terminal THF ligand, and

<sup>a</sup>Davenport Chemical Research Laboratories, Department of Chemistry, University of Toronto, 80 St. George Street, Toronto, Ontario, Canada, M5S 3H6.

E-mail: dsong@chem.utoronto.ca; Fax: +1 416 978 7013; Tel: +1 416 978 7014

<sup>b</sup>Department of Chemistry and Biochemistry, University of Windsor, 401 Sunset Avenue, Windsor, ON, Canada, N9B 3P4

†Electronic supplementary information (ESI) available: For crystallographic data in CIF and further computation details. CCDC 935013–935017. For ESI and crystallographic data in CIF or other electronic format see DOI: 10.1039/c3dt51063h

Scheme 2 Synthesis of **2**.

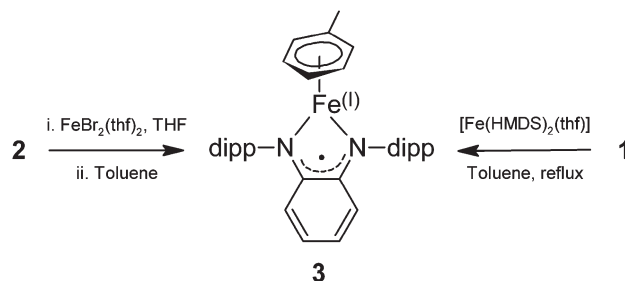
**Fig. 1** Molecular structure of **2** (50% probability thermal ellipsoids). All hydrogen atoms and the iso-propyl groups are omitted and only one orientation of the disordered portion is shown for clarity. Selected bond lengths (Å): C30–N2 1.396(2), C25–N1 1.395(2), C30–C25 1.439(2), C25–C26 1.399(3), C26–C27 1.400(3), C27–C28 1.384(3), C28–C29 1.397(3), C29–C30 1.394(3); selected bond angles (°): O1–Li1–O2 114.09(16), O1–Li1–N2 122.92(17), O2–Li1–N2 106.25(15), O1–Li1–N1 128.91(17), O2–Li1–N1 99.46(15), N1–Li1–N2 78.65(12), O3–Li2–N2 121.89(18), O3–Li2–N1 154.4(2), N1–Li2–N2 82.72(13), O3–Li2–O2 95.62(15), N2–Li2–O2 94.64(15), N1–Li2–O2 88.57(13).

another oxygen donor atom from a bridging THF ligand occupying the four coordination sites. The coordination geometry around Li2 is better described as trigonal pyramidal with N1 and N2 from the chelating ligand and O3 from the terminal THF ligand occupying the trigonal base and O2 from the bridging THF ligand occupying the apical position. Within the trigonal base, the N1–Li2–O3, N1–Li2–N2, and N2–Li2–O3 angles are 154.4(2), 82.7(1), and 121.9(2)°, respectively. The dihedral angle between the phenylenediamide plane and the Li1–N1–N2 plane is ~74°, while that between the phenylenediamide plane and the Li2–N1–N2 plane is ~24°. The analogous monomeric dilithium complexes of *N,N'*-disilyl-*o*-phenylenediamide derivatives reported by Lappert and coworkers<sup>29</sup> have both a three-coordinate and a four-coordinate lithium centre, with one and two terminal THF ligands, respectively. The solution <sup>1</sup>H NMR spectrum of **2** reveals a symmetrical molecule in solution, *i.e.*, the protons of the dipp groups on both sides of the phenylenediamide plane show only one set of <sup>1</sup>H resonances. The three THF ligands only show one set of resonances at 1.17 and 3.25 ppm, similar to those reported by Lappert. The single

peak in the solution <sup>7</sup>Li NMR spectrum at 2.62 ppm also suggests that the two lithium centres are equivalent in solution. The N2–C30 and N1–C25 bond lengths are 1.396(2) and 1.395(2) Å, respectively, consistent with the typical C–N single bond in phenylenediamide complexes. The bridging coordination mode and the distorted tetrahedral local geometry of the two nitrogen atoms also suggest that both nitrogen atoms are sp<sup>3</sup> hybridized amido nitrogen with two lone pairs on each.

### Fe coordination chemistry of **2**

Compound **2** reacts with FeBr<sub>2</sub>(thf)<sub>2</sub> in THF at –60 °C to afford a navy blue solution. Our efforts to determine the identity of the blue species have been unsuccessful. However, the addition of toluene to the reaction mixture after the removal of solvents yields compound **3** (Scheme 3), the formation of which is accompanied by a rapid colour change to purple. Compound **3** can also be synthesized by reacting **1** with [Fe(HMDS)<sub>2</sub>(thf)] in toluene at elevated temperatures. In the <sup>1</sup>H NMR spectrum, three resonances at 5.41, 5.19, and 4.91 ppm (triplet, doublet, triplet) suggest the presence of highly shielded arene protons, consistent with an η<sup>6</sup>-toluene adduct of iron.<sup>30,31</sup> An X-ray diffraction study revealed the two-legged ‘piano stool’ structure of **3** (Fig. 2). The C30–N2 and C25–N1 bond lengths are 1.361(2) and 1.366(2) Å, respectively, shorter than those in **2**, but longer than a typical C–N double bond. The C25–C30 bond length (1.419(2) Å) in **3** is shorter than that in **2** (1.439(2) Å). The bond lengths in the phenylene backbone reveal subtle dearomatization: the average C<sub>β</sub>–C<sub>γ</sub> bond length in **3** is 1.377(2) Å, and the average C<sub>α</sub>–C<sub>β</sub> bond length is 1.411(2) Å. The metric parameters suggest that the *N,N*-chelating ligand may contain radical character with the unpaired electron antiferromagnetically coupled with that of the low spin iron(i) centre. Wieghardt and coworkers have demonstrated that when ambiguous, the oxidation states of metal and bis-*o*-substituted N or O-donor ligands may be assigned based on high-quality single crystal X-ray diffraction data.<sup>32</sup> The metric parameters of the chelating ligand in **2** compare well with literature examples of *o*-diiminoquinonate complexes characterized crystallographically.<sup>15,17,20–25,33</sup> To obtain further information on the electronic structure of compound **2**, we carried out DFT calculations. Our calculations showed that the model with antiferromagnetically coupled Fe(i) and open-shell ligand is more stable than the closed shell model with Fe(0) and a neutral diimine ligand. The spin density on the Fe

Scheme 3 Two synthetic routes to **3**.

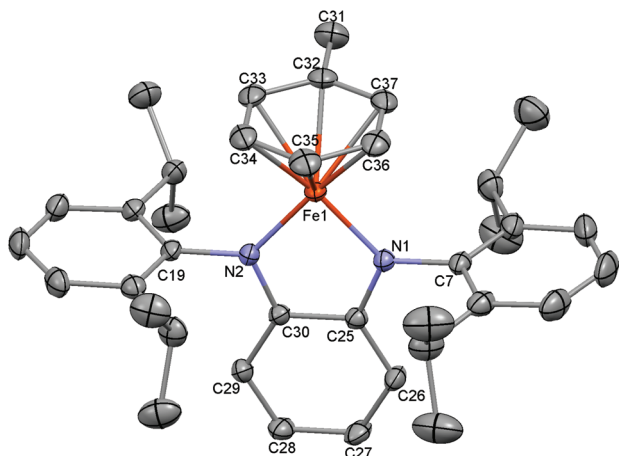
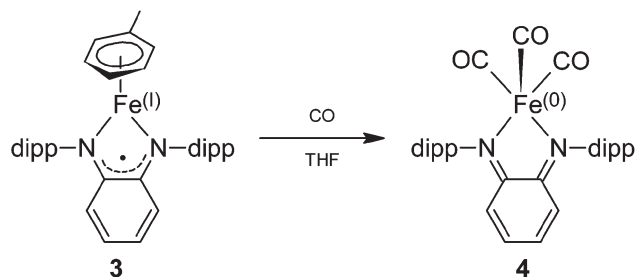


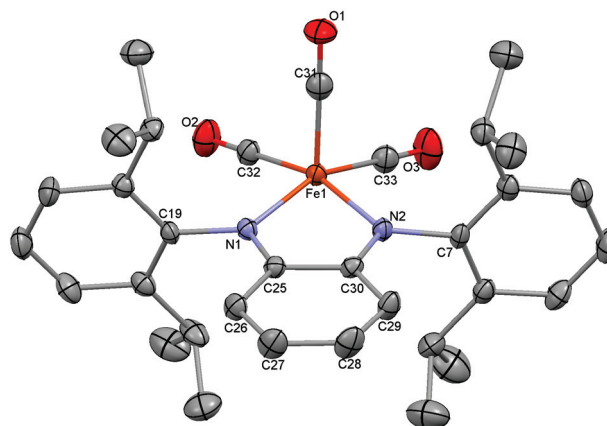
**Fig. 2** Molecular structure of **3** (50% probability thermal ellipsoids). All hydrogen atoms are omitted for clarity. Selected bond lengths (Å) and angles (°): Fe–N1 1.880(1), Fe–N2 1.882(1), C25–N1 1.366(2), C30–N2 1.361(2), C25–C26 1.409(2), C26–C27 1.379(2), C27–C28 1.407(2), C28–C29 1.374(2), C29–C30 1.413(2), C30–C25 1.419(2), C32–C33 1.419(2), C33–C34 1.409(3), C34–C35 1.414(3), C35–C36 1.415(2), C36–C37 1.409(3), C37–C32 1.415(2); N2–C30–C25 113.2(1), N1–C25–C30 112.8(1), N2–Fe1–N1 82.68(5).

centre is 0.734 in the antiferromagnetically coupled model, smaller than 1.00, which is reasonable due to covalent bonding and orbital mixing between the metal and the ligand.<sup>21</sup> The simplified orbital spin density analysis (*i.e.*, if the spin density is lower than 0.5, the orbital is considered empty; if the spin density is greater than 0.5, the orbital is considered occupied) showed the following electronic configuration on Fe: empty  $d_{yz}$ , singly occupied  $d_{xy}$ , and doubly occupied  $d_{xz}$ ,  $d_{x^2-y^2}$ , and  $d_{z^2}$  orbitals. Although the actual electronic structure is somewhere in between the two extremes, *i.e.*, Fe(0) with a neutral diimine ligand and Fe(I) with a mono-anionic radical ligand, such an approximation in orbital spin density analysis indicates that the actual structure is closer to the latter extreme in the continuum. Overall, the transformation from **2** to **3** involves reduction of Fe(II) to Fe(I) by the electron-rich dilithium diamide complex, accompanied by coordination of the oxidized ligand. Chirik *et al.* have characterized a series of complexes with a general formula  $[\text{ArN}=\text{C}(\text{Me})\text{C}(\text{Me})=\text{NAr}]\text{Fe}(\eta^6\text{-arene})$ , *via* the reduction of dichloro  $[\text{ArN}=\text{C}(\text{Me})\text{C}(\text{Me})=\text{NAr}]\text{Fe}(\text{II})$  complexes with sodium amalgam in the presence of various arenes.<sup>31</sup> When the Ar group in Chirik's complexes is 2,6-diisopropylphenyl and the  $\eta^6\text{-arene}$  is toluene, the average C=N bond length is 1.359(3) Å, which is similar to that in **3**. The average C–C bond length of the  $\eta^6\text{-toluene}$  in **3** is 1.414(3) Å, nearly identical to that in Chirik's complex (1.412(5) Å).

When a THF solution of **3** is stirred under an atmosphere of CO, the toluene ligand can be displaced to yield **4**, in which three CO ligands are coordinated to the iron centre (Scheme 4). The diagnostic NMR data for **4** are the absence of the shielded  $\eta^6\text{-toluene}$  peaks from the  $^1\text{H}$  NMR spectrum and the presence of a highly deshielded carbonyl peak at 210 ppm in the  $^{13}\text{C}$  NMR spectrum. The crystal structure of **4** is shown



**Scheme 4** Synthesis of **4**.

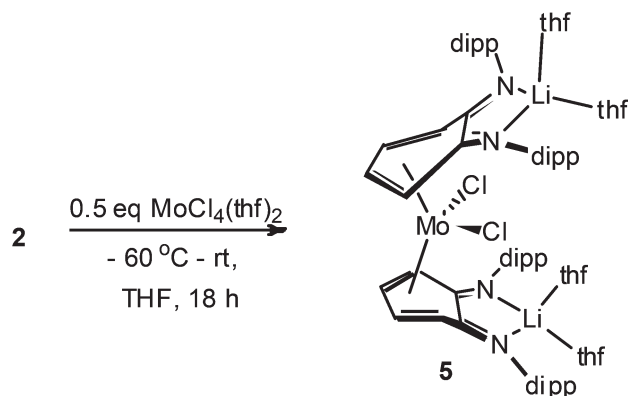


**Fig. 3** Molecular structure of **4** (50% probability thermal ellipsoids). All hydrogen atoms are omitted for clarity. Selected bond lengths (Å) and angles (°): Fe1–N2 1.914(2), Fe1–N1 1.911(2), Fe1–C31 1.799(2), C31–O1 1.132(3), C30–N2 1.353(3), C25–N1 1.354(3), C25–C26 1.414(3), C26–C27 1.367(4), C27–C28 1.416(3), C28–C29 1.369(4), C29–C30 1.414(3), C25–C30 1.425(3); N2–C30–C25 113.2(2), N1–C25–C30 113.1(2), N1–Fe–N2 81.15(8).

in Fig. 3. The C25–N1 and C30–N2 bond lengths are 1.354(3) and 1.353(3) Å, respectively, and are marginally shorter than those in **3** but not statistically different. To elucidate the electronic structure of **4**, we performed DFT calculations. The spin-unrestricted and restricted models from DFT are similar in energy. In the spin-unrestricted model, the spin density on the Fe centre is 0.391. The simplified orbital spin density analysis on such a structure showed the following electronic configuration on Fe: empty  $d_{yz}$ , and doubly occupied  $d_{xz}$ ,  $d_{xy}$ ,  $d_{x^2-y^2}$ , and  $d_{z^2}$  orbitals, consistent with Fe(0). Such an approximation indicates that the actual structure is closer to the Fe(0) with a neutral diimine ligand extreme in the continuum. Presumably the better  $\pi$ -acceptor ligand, CO induced further electron transfer from the chelating ligand to the metal centre.

## Mo coordination chemistry of **2**

The reaction of **2** with 0.5 equiv. of  $\text{MoCl}_4(\text{thf})_2$  afforded emerald green compound **5** (Scheme 5), which is diamagnetic as evidenced by its sharp NMR spectra within the normal chemical shift range. The  $^7\text{Li}$  NMR experiment reveals the presence of lithium in the product: one singlet at 1.37 ppm, which is upfield shifted compared to the singlet at 2.62 ppm present

Scheme 5 Synthesis of **5**.

in the starting material **2**. In the  $^1\text{H}$  NMR spectrum, the conversion of **2** to **5** is accompanied by the disappearance of multiplets at 6.57 and 6.33 ppm corresponding to the phenylene protons of the starting material, and the appearance of resonances at 5.30, 4.88, 2.69, and 2.30 ppm hinting the vanished aromaticity of the phenylene ring.

The solid state structure of **5** was confirmed by a single-crystal X-ray diffraction study. As shown in Fig. 4, the molecule is  $C_2$  symmetric with a crystallographically imposed  $C_2$  axis bisecting the Cl–Mo–Cl' angle, relating a pair of chloride ligands and a pair of organic ligands, respectively. Interestingly, instead of coordinating to the molybdenum centre, the two nitrogen donor atoms of each organic ligand are coordinating to a lithium centre, which is further ligated by two THF molecules *via* the oxygen donor atoms. The C25–N1 and C30–N2 bond lengths are 1.314(7) and 1.309(7) Å, respectively, which are more similar to C–N bond lengths found in typical diimine complexes ( $\sim 1.28$  Å)<sup>34</sup> than those found in typical

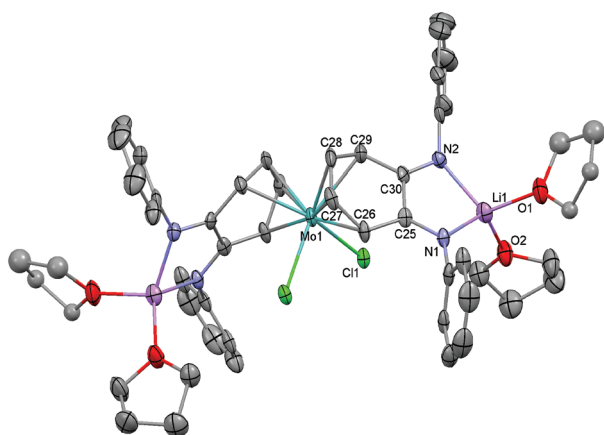


**Fig. 4** Molecular structure of **5** (50% probability thermal ellipsoids). All hydrogen atoms and the isopropyl groups are omitted and only one orientation of the disordered portion is shown for clarity. Selected bond lengths (Å) and angles (°): Mo1–Cl1 2.522(1), Mo1–C26 2.342(5), Mo1–C27 2.214(5), Mo1–C28 2.207(6), Mo1–C29 2.363(6), C25–N1 1.314(7), C30–N2 1.309(7), N1–Li1 2.032(8), N2–Li1 2.043(9), C25–C26 1.425(6), C26–C27 1.437(7), C27–C28 1.405(6), C28–C29 1.444(7), C29–C30 1.428(9), C25–C30 1.498(6); Cl1–Mo–Cl1' 90.60(4).

diamide complexes ( $\sim 1.38$ – $1.42$  Å).<sup>35</sup> The short C–N and long C–C bond (C25–C30 1.498(6) Å) lengths are consistent with a neutral diimine ligand.

The molybdenum centre is sandwiched between two central  $C_6$  rings of two diimine ligands. Both  $C_6$  rings coordinate to the molybdenum centre in an  $\eta^4$  fashion. Such a coordination mode for a pda-type ligand is complementary to one mode reported for an  $\text{MoRu}_2$  trimetallic complex by Mealli *et al.*, in which Mo is coordinated  $\eta^4$  to pda through both amide nitrogens and both  $\alpha$ -carbons.<sup>36</sup> A more similar coordination mode has been observed in Mo–Al bimetallic complexes of the  $[o\text{-C}_6\text{H}_4\text{-(NSiMe}_3)_2]^{2-}$  ligand reported by Boncella and co-workers.<sup>37</sup> Distinct from this literature example, the  $\eta^4$ - $C_6$  ring in compound **5** is far from planar; the ring folds about the C26–C29 vector with a dihedral angle of  $\sim 30^\circ$  into a boat conformation, suggesting the diminishing conjugation between the coordinating portion (C26, C27, C28 and C29) and the remaining portion of the  $C_6$  ring. Such folding is similar to that observed in the Mo-( $\eta^4$ -phenazine) type of complexes reported by Parkin and coworkers.<sup>38</sup> The coordination environment around the molybdenum centre in **5** is reminiscent of the pseudo- $C_2$  symmetric  $(\text{Me}_3\text{P})_2\text{Mo}(\eta^4\text{-butadiene})_2$ ,<sup>39</sup> in that both compounds bear two *syn* diene ligands and two mutually *cis* monodentate ligands, and have an overall coordination number of six. The P–Mo–P angle in  $(\text{Me}_3\text{P})_2\text{Mo}(\eta^4\text{-butadiene})_2$  is  $98^\circ$ , slightly larger than the  $91^\circ$  Cl–Mo–Cl angle in compound **5**, likely due to sterics. An additional structural parameter that has been used to describe butadiene ligand geometry is  $\Phi$ , the dihedral angle between the butadiene plane and the plane containing both outer carbons and the metal centre ( $C_o\text{--}M\text{--}C_o'$ ).<sup>40</sup> In this respect, **5** ( $\sim 78^\circ$ ) closely resembles  $(\text{Me}_3\text{P})_2\text{Mo}(\eta^4\text{-butadiene})_2$  ( $\sim 83^\circ$ ).

Butadiene complexes are most often compared to the two canonical resonance forms as shown in Chart 1, the neutral diene ( $L_2$ ) on a metal and the metallacyclopentene ( $LX_2$ ) on a metal formally oxidized by two electrons.<sup>41</sup> Metallacyclopentenes feature a negative  $\Delta d$ , where  $\Delta d = \text{avg. } M\text{--}C_o \text{ bond length} - \text{avg. } M\text{--}C_i \text{ bond length}$ . Another characteristic feature of metallacyclopentenes is that  $C_i\text{--}C_i$  bonds are shorter than  $C_i\text{--}C_o$  bonds. In  $L_2$  butadiene complexes however,  $\Delta d$  is positive and all butadiene C–C bond lengths are similar.<sup>41</sup> The  $\Delta d$  parameter for **5** is 0.142(6) Å and the  $C_i\text{--}C_i$  (1.405(6) Å) and  $C_i\text{--}C_o$  (avg. 1.440(7) Å) bond lengths in **5** are statistically similar. Similar  $\eta^4$ -butadiene C–C bond lengths and the positive  $\Delta d$  are indicative of an  $L_2$  butadiene complex. Similarly, in  $[(\text{Me}_3\text{P})_2\text{Mo}(\eta^4\text{-butadiene})_2]$  the  $\Delta d$  (0.065 Å average of both

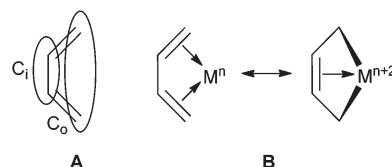


**Chart 1** A: Labelling of inner ( $C_i$ ) and outer ( $C_o$ ) butadiene carbons; B: two extreme resonance forms of a generic diene complex.



ligands) is positive, and the average C<sub>i</sub>–C<sub>i</sub> (1.398(5) Å) and C<sub>i</sub>–C<sub>o</sub> (1.413(5) Å) distances are statistically indistinguishable. Although the actual structure of the η<sup>4</sup>-ligand in **5** still lies between the two extreme resonance forms, all the metric parameters from the crystal structure of **5** suggest that the L<sub>2</sub> resonance form of the η<sup>4</sup>-ligand contributes more to the overall structure. In the resonance structure with an L<sub>2</sub> type η<sup>4</sup>-ligand, the molybdenum centre has a formal oxidation state of zero. The reaction between **2** and MoCl<sub>4</sub>(thf)<sub>2</sub> could then be rationalized as the reduction of Mo(IV) to Mo(0) by 2 equiv. of **2** where the diamido ligand is oxidized into diimine.

When the reaction between **2** and MoCl<sub>4</sub>(thf)<sub>2</sub> is quenched within 2 h, an emerald green paramagnetic species **6** can be isolated by a rapid crystallization. Alternatively, **6** can be synthesized by reacting **1** with EuCl<sub>3</sub>(dme)<sub>2</sub>. The crystal structure of **6** is shown in Fig. 5. The molecule of **6** has a crystallographically imposed C<sub>2</sub> symmetry along the Li1–O1 direction. The lithium centre adopts a trigonal planar coordination geometry with two nitrogen donor atoms from the chelating ligand and an oxygen donor atom from an ether ligand occupying the three coordination sites. The N,N'-chelate ligand has a net charge of –1, *i.e.*, a radical bound to a relatively innocent Li ion. Interestingly, the N1–C13 and C14–C15 bond lengths (1.341(3) and 1.364(4) Å, respectively) are shorter than their counterparts in **3**, while the C13–C14 and C13–C13' bond lengths (1.429(3) and 1.471(5) Å, respectively) are longer than their counterparts in **3**. The C15–C15' bond length (1.400(5) Å) is similar to its counterpart in **3**.

### EPR data for **6**

The solid state EPR spectrum of compound **6** (Fig. 6) revealed a sharp singlet ( $\Delta H = 2.8$  G, with a Lorentzian profile) at  $g = 2.0030$ , close to the free electron value of 2.0036 consistent with an organic radical with little anisotropy and where spin-orbit coupling is negligible. The deep green solution of **6** in

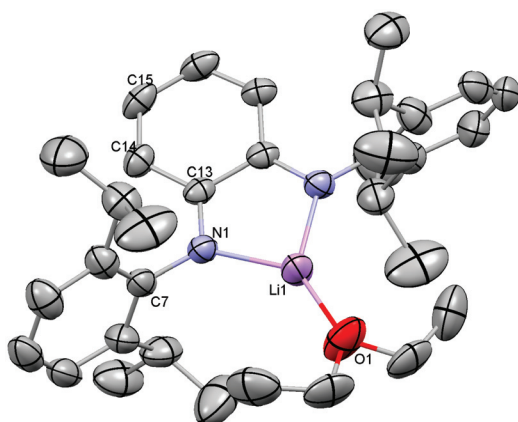


**Fig. 5** Molecular structure of **6** (30% probability thermal ellipsoids). Hydrogen atoms are omitted and only one orientation of the disordered portions is shown for clarity. Selected bond lengths (Å) and angles (°): Li1–O1 1.882(7), Li1–N1 1.974(6), N1–C13 1.341(3), C13–C13' 1.478(5), C13–C14 1.422(4), C14–C15 1.364(4), C15–C15' 1.400(6); O1–Li1–N1 136.7(2), N1–Li1–N1' 86.7(3), C13–N1–C7 117.8(2), C13–N1–Li1 109.4(2), C7–N1–Li1 132.9(2).

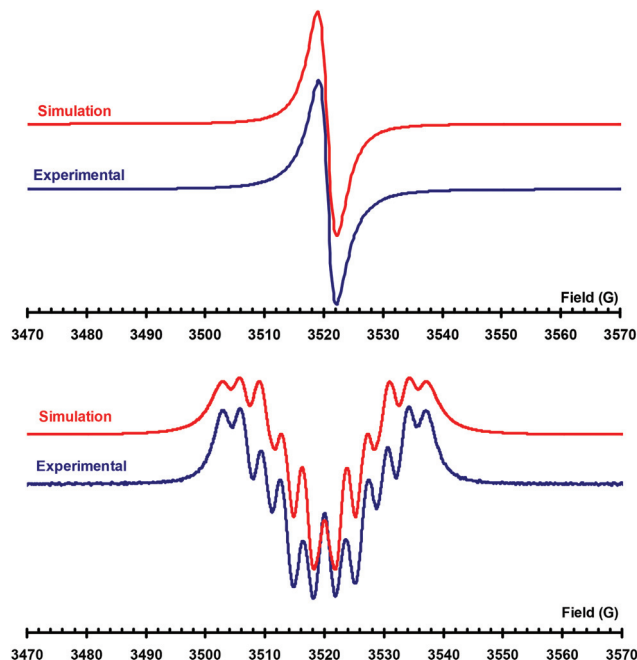


**Fig. 6** EPR spectra of **6** in the solid state (top) and in toluene solution (bottom) at ambient temperature.

toluene at room temperature revealed a multiplet pattern consistent with delocalisation over the phenylenediamine framework as well as the Li atom. The observation of hyperfine coupling to <sup>7</sup>Li is consistent with ion-pairing in solution and retention of the molecular structure determined from X-ray diffraction. In contrast, the Zn complex of the open-shell neopentyl-substituted phenylenediamide derivative showed a broad EPR signal at room temperature in a THF solution with unresolved hyperfine coupling.<sup>33</sup>

The spin density distribution based on coupling to two chemically equivalent <sup>14</sup>N nuclei and two pairs of chemically distinct <sup>1</sup>H nuclei (along with <sup>7</sup>Li coupling) is consistent with a π-delocalised radical based on the *ortho*-phenylene framework and in good agreement with the computationally determined spin distribution. An estimate of the spin density distribution at C can be made based on McConnell's empirical relationship<sup>42</sup> ( $a_H = Q_{CH}\rho_C$  where  $Q_{CH} = 22.5$  G). Whilst similar relationships are proposed to exist for N ( $a_N = Q_N\rho_N$  and  $Q_N = 26.9$  G),<sup>43</sup> the behaviour for N appears more complex.<sup>43</sup> Nevertheless the EPR data are consistent with a ligand-based π-radical (Fig. 7).

## Conclusion

A dilithium complex (**2**) of *N,N'*-bis(2,6-diisopropylphenyl)-*o*-phenylenediamide was synthesized and its coordination behaviour towards halides of iron and molybdenum was investigated. Rather than forming mid-valent transition metal complexes with π-donating diamido ligands, the dilithium diamide complex **2** reduced both iron and molybdenum. In

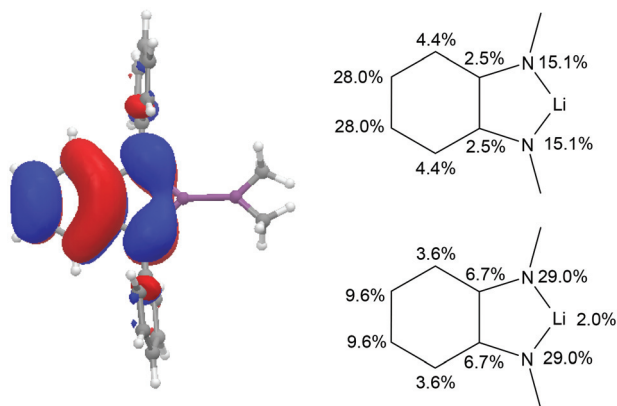


**Fig. 7** Singly occupied molecular orbital (left) for model compound  $[C_6H_4(NPh)_2LiOMe_2]$  (B3LYP/6-311G\*\*) and estimated (right, top) and computed (B3LYP/6-31G\*) spin density (right bottom) for **6**.

the case of Fe, the addition of external  $\pi$ -acceptor ligands, toluene and CO, facilitated the formation and isolation of low-valent Fe complexes **3** and **4**, respectively. In the case of Mo, the  $C_6$  ring of the resulting  $pda^0$  ligand lost its planarity and acted as a  $\pi$ -acceptor ligand that coordinated to the resulting low-valent Mo centre in an  $\eta^4$  fashion to form **5**. The  $1e^-$  oxidation of **2** by Mo(IV) or Eu(III) yielded complex **6** featuring an open-shell ligand supported by a lithium cation. Complex **6** showed typical ligand-based radical character with delocalized spin density. The coordination chemistry of **2** towards other metals is underway in our laboratory.

## Experimental section

### General considerations

All operations were performed using standard Schlenk techniques under a nitrogen atmosphere, or in a nitrogen-filled MBraun glovebox.  $FeBr_2(thf)_2$ ,<sup>44</sup>  $[Fe(HMDS)_2(thf)]$ ,<sup>45</sup>  $MoCl_4(thf)_2$ ,<sup>46</sup>  $EuCl_3(dme)_2$ ,<sup>47</sup> and **1**<sup>27</sup> were prepared according to literature procedures. Glassware was either flame-dried or dried overnight in a 160 °C oven prior to use except for NMR tubes which were dried overnight in a 60 °C oven. Carbon monoxide was purchased from Linde and used without further purification,  $n$ -BuLi (1.6 M in hexanes) was purchased from Aldrich. THF, toluene, ether, and benzene- $d_6$  were dried over Na/benzophenone, distilled under nitrogen, and stored over activated molecular sieves. Room temperature solid state and toluene solution EPR spectra of **6** were recorded on a Bruker EMXplus X-band EPR spectrometer and spectra simulated using Winsim.<sup>48</sup> The  $^1H$ ,  $^7Li$ , and  $^{13}C$  NMR spectra were recorded on either a Varian 400 MHz, an Agilent 500 MHz, or an Agilent 600 MHz NMR spectrometer. All chemical shifts are reported in ppm relative to the residual protio-solvent peaks;  $^7Li$  NMR spectra are referenced externally using 9.7 M LiCl in  $D_2O$ . FT-IR spectra were recorded on a Perkin Elmer Spectrum One FT-IR spectrometer. Elemental analysis was performed by ANALEST at the University of Toronto.

### $Li_2L(thf)_3$ , **2**

$N,N'$ -Bis(2,6-diisopropylphenyl)- $o$ -phenylenediamine (0.50 g, 1.2 mmol) was dissolved in THF (5 mL) and cooled to  $-70$  °C. A hexanes solution of  $n$ -butyl lithium (1.5 mL, 1.6 M) was added dropwise. The reaction mixture was removed from the cooling bath and stirred for 90 min, during which a precipitate formed. Hexane (10 mL) was added and the mixture cooled to  $-25$  °C. The precipitate was collected on a frit and was washed with cold hexanes. Drying *in vacuo* left a light yellow powder (0.528 g, 67%), which was stored at  $-25$  °C. Not only is this material extremely air-sensitive, but it also decomposes under prolonged vacuum at room temperature. Consequently no satisfactory analytical data were obtained. Single crystals were obtained from a  $C_6D_6$  solution sitting at room temperature for days.  $^1H$  NMR (400 MHz, 25 °C,  $C_6D_6$ )  $\delta$  7.39 (d,  $J$  = 7.6 Hz, 4H), 7.23 (t,  $J$  = 7.6 Hz, 2H), 6.57 (m, 2H), 6.33 (m, 2H), 3.43 (sept,  $J$  = 7.1 Hz, 4H), 3.25 (m, 12H), 1.38 (d,  $J$  = 6.8 Hz, 12H), 1.29 (d,  $J$  = 7 Hz, 12H), 1.17 (m, 12H).  $^{13}C\{^1H\}$  NMR (100.58 MHz,  $C_6D_6$ , 25 °C)  $\delta$  153.56, 148.72, 144.36, 121.20, 115.02, 112.14, 68.86, 29.92, 25.78, 25.69, 25.23.  $^7Li$  NMR (233 MHz, 25 °C,  $C_6D_6$ ):  $\delta$  2.62.

### $LiFe(\eta^6\text{-toluene})$ , **3**, method A

$Li_2L(thf)_3$  (0.10 g, 0.15 mmol) was dissolved in THF (2 mL) and cooled to an internal temperature of  $-60$  °C. The resulting yellow solution was added smoothly to a  $-60$  °C suspension of  $FeBr_2(thf)_2$  (0.055 g, 0.15 mmol) in THF (1 mL). The resulting mixture was allowed to warm to room temperature with stirring for 24 h. Volatiles were removed under vacuum, leaving a navy blue oil. The addition of toluene (3 mL) resulted in a purple solution which was stirred for 1 h. The mixture was filtered through Celite and dried under vacuum. The residue was dissolved in hexanes (1 mL) and cooled to  $-25$  °C, resulting in the precipitation of **3**. The supernatant was decanted, leaving a purple solid (0.054 g, 61%) which was dried *in vacuo*. Trace LiBr could be removed by recrystallization from hexanes. NMR data for **3** obtained this way are identical to those obtained by method B.

### $LiFe(\eta^6\text{-toluene})$ , **3**, method B

Solid  $H_2L$  (0.47 g, 1.1 mmol) was added to a solution of  $Fe(HMDS)_2(thf)$  (0.45 g, 1.0 mmol) in toluene (15 mL). The mixture quickly turned purple and was refluxed for 16 h. After cooling to room temperature, volatiles were removed under vacuum at 50 °C, leaving a purple solid which was dissolved in hexanes and filtered through Celite. The filtrate was concentrated and cooled to  $-25$  °C, which caused formation of purple crystals which were collected on a frit and washed with cold hexanes, yielding **3** (0.29 g, 0.50 mmol, 50%). Single-crystals suitable for XRD studies were grown by slow evaporation of a hexanes solution at room temperature. Anal. Calcd for  $C_{37}H_{46}N_2Fe$ : C, 77.34; H, 8.07; N, 4.88. Found: C, 77.09; H, 7.94; N, 4.88.  $^1H$  NMR (500 MHz, 25 °C,  $C_6D_6$ ):  $\delta$  7.49 (t,  $J$  = 7.5 Hz, 2H), 7.41 (d,  $J$  = 7.5 Hz, 4H), 6.60 (m, 2H), 6.44 (m, 2H), 5.41 (t,  $J$  = 5.7 Hz, 1H), 5.19 (d,  $J$  = 6.1 Hz, 2H), 4.91 (t,  $J$  = 6 Hz,

2H), 3.28 (sept,  $J = 6.9$  Hz, 4H), 2.10 (s, 3H), 1.46 (d,  $J = 6.9$  Hz, 12H), 0.88 (d,  $J = 6.9$  Hz, 12H).  $^{13}\text{C}\{^1\text{H}\}$  NMR (125.72 MHz, 25 °C,  $\text{C}_6\text{D}_6$ ):  $\delta$  153.62, 152.01, 143.84, 126.10, 124.20, 119.14, 115.17, 97.58, 83.43, 82.77, 81.37, 28.72, 26.46, 24.74, 19.81.

#### **$\text{LFe}(\text{CO})_3$ , 4**

$\text{LFe}(\eta^6\text{-toluene})$  (70 mg, 0.12 mmol) was dissolved in THF (2 mL) in a Schlenk bomb. The solution was degassed before one atmosphere of carbon monoxide was introduced. The solution was stirred for 16 h at room temperature. The solvent was removed under vacuum and the purple residue was extracted into hexanes and filtered through Celite. Concentration of the filtrate and storage at  $-25$  °C yielded **4** as purple crystals. The supernatant was decanted and the solid dried *in vacuo*. (22 mg, 32%). Single crystals of **4** were grown by slow evaporation of a room temperature hexanes solution. Anal. Calcd for  $\text{C}_{33}\text{H}_{38}\text{N}_2\text{O}_3\text{Fe}$ : C, 69.96; H, 6.76; N, 4.94. Found: C, 70.01; H, 6.97, N, 4.91. IR(nujol,  $\text{cm}^{-1}$ )  $\nu_{\text{CO}}$ : 2049, 1985, 1977.  $^1\text{H}$  NMR (600 MHz, 25 °C,  $\text{C}_6\text{D}_6$ ):  $\delta$  7.29 (t,  $J = 7.9$  Hz, 2H), 7.22 (d,  $J = 7.7$  Hz, 4H), 6.62 (m, 4H), 2.86 (sept,  $J = 7.1$  Hz, 4H), 1.34 (d,  $J = 7$  Hz, 12H), 0.94 (d,  $J = 6.7$  Hz, 12H).  $^{13}\text{C}\{^1\text{H}\}$  NMR (150.9 MHz,  $\text{C}_6\text{D}_6$ , 25 °C):  $\delta$  209.99, 155.00, 150.73, 142.42, 128.04, 124.42, 123.31, 117.20, 28.62, 25.62, 24.69.

#### **$(\text{LiL})_2\text{MoCl}_2(\text{thf})_4$ , 5**

To a suspension of  $\text{MoCl}_4(\text{thf})_2$  (36 mg, 0.095 mmol) in THF (1 mL) which was precooled to  $-60$  °C was slowly added a solution of  $\text{Li}_2\text{L}(\text{thf})_3$  (0.125 g, 0.19 mmol) in THF (2 mL) which was also precooled to  $-60$  °C. The mixture immediately turned emerald green and was removed from the cold well and stirred for 18 h at ambient temperature. Volatiles were removed *in vacuo* and toluene (4 mL) was added. The solution was filtered through Celite and dried under vacuum. The residue was recrystallized from a mixture of THF and hexanes at  $-25$  °C to yield green crystals, which were collected by vacuum filtration and dried under vacuum yielding **5** as a green powder (61 mg, 56%). Single crystals for XRD studies were grown by cooling a THF solution to  $-25$  °C.  $^1\text{H}$  NMR (400 MHz, 25 °C,  $\text{C}_6\text{D}_6$ )  $\delta$  7.33 (dd,  $J = 7.6$  Hz,  $J = 1.4$  Hz, 2H), 7.24 (dd,  $J = 5.6$  Hz,  $J = 1.4$  Hz, 2H), 7.22 (dd,  $J = 5.6$  Hz,  $J = 1.6$  Hz, 2H), 7.15 (dd overlapped with solvent peak,  $J = 1.8$  Hz, 2H), 7.10 (td,  $J = 7.6$  Hz,  $J = 2.9$  Hz, 4H), 5.30 (td,  $J = 6.8$  Hz,  $J = 1.4$  Hz, 2H), 4.88 (dd,  $J = 6.8$  Hz,  $J = 2.4$  Hz, 2H), 4.20 (sept,  $J = 6.8$  Hz, 2H), 3.40 (m, 6H), 3.31 (m, 16H), 2.69 (dt,  $J = 7.4$  Hz,  $J = 2.6$  Hz, 2H), 2.30 (dd,  $J = 6.6$  Hz,  $J = 1.0$  Hz, 2H), 1.90 (d,  $J = 6.7$  Hz, 6H), 1.51 (d,  $J = 6.8$  Hz, 6H), 1.43 (d,  $J = 6.8$  Hz, 6H), 1.30 (m, 18H), 1.17 (d,  $J = 6.8$  Hz, 6H), 1.04 (d,  $J = 6.8$  Hz, 6H).  $^{13}\text{C}\{^1\text{H}\}$  NMR (100.58 MHz,  $\text{C}_6\text{D}_6$ , 25 °C): 167.91, 164.86, 147.03, 146.61, 142.32, 141.92, 140.20, 139.80, 124.95, 124.70, 124.07, 123.87, 123.70, 123.59, 86.76, 86.38, 76.56, 68.59, 61.12, 28.94, 28.78, 28.17, 27.78, 26.22, 25.65, 25.05, 24.83, 24.76, 24.73, 24.55, 24.11, 23.07, 14.69, 14.62.  $^7\text{Li}$  NMR (233 MHz, 25 °C,  $\text{C}_6\text{D}_6$ ):  $\delta$  1.37. Anal. Calcd for  $\text{C}_{76}\text{H}_{108}\text{N}_4\text{O}_4\text{MoLi}_2\text{Cl}_2$ : C, 69.02; H, 8.23; N, 4.23. Found: C, 68.78; H, 8.00; N, 4.41.

#### **$\text{LiL}(\text{Et}_2\text{O})$ , 6**

**6** was first isolated as a minor product in the reaction of  $\text{MoCl}_4(\text{thf})_2$  with two equivalents of  $\text{Li}_2\text{L}(\text{thf})_3$  when the reaction time was shortened from 18 h to 2 h. However, **6** could be synthesized more reliably and in better yield from the reaction of  $\text{Li}_2\text{L}(\text{thf})_3$  with  $\text{EuCl}_3(\text{dme})_2$ . In a glove box cold well, a solution of  $\text{Li}_2\text{L}(\text{thf})_3$  (69 mg, 0.11 mmol) in THF (2 mL) was cooled to an internal temperature of  $-70$  °C. This solution was smoothly added to a similarly cooled suspension of  $\text{EuCl}_3(\text{dme})_2$  (46 mg, 0.11 mmol) in THF (2 mL). The mixture turned emerald green instantly, was allowed to warm to 28 °C, and was then stirred for 18 h. Volatiles were removed *in vacuo*, ether (5 mL) was added, and the mixture was filtered. After removal of ether and recrystallization from cold pentane, green crystals of  $\text{LiL}(\text{Et}_2\text{O})$  (18 mg, 34%) were isolated, and stored at  $-25$  °C. Anal. Calcd for  $\text{C}_{34}\text{H}_{48}\text{N}_2\text{OLi}$ : C, 80.43; H, 9.53; N, 5.52. Found: C, 79.78; H, 9.46; N, 5.49.

#### **X-ray crystallography**

All crystals were mounted on the tip of a MiTeGen MicroMount and the single-crystal X-ray diffraction data were collected on a Bruker Kappa Apex II diffractometer. All data were collected with graphite-monochromated Mo  $\text{K}\alpha$  radiation ( $\lambda = 0.71073$  Å) at 150 K controlled by an Oxford Cryostream 700 series low temperature system. The diffraction data were processed with the Bruker Apex 2 software package.<sup>49</sup> Raw data were processed and multiscan absorption corrections were applied using the Bruker Apex 2 software package.<sup>49</sup> All structures were solved by the direct methods and refined using SHELXTL V6.14.<sup>50</sup> Compounds **2**, **3**, **4**, **5** crystallized in the monoclinic space groups  $P2_1$ ,  $P2_1/n$ ,  $P2_1/c$ , and  $C2/c$ , respectively, while **6** crystallized in the tetragonal space group  $P4_32_12$ . The disordered THF ligand in **5** and the ether ligand and isopropyl groups in **6** were modelled successfully. The residual diffuse electron density from disordered, unidentified solvent molecules in the lattice of **5** was removed with the SQUEEZE function of the PLATON program<sup>51</sup> and their contributions were not included in the formula. All non-hydrogen atoms were refined anisotropically, except for the disordered portions. In all structures hydrogen atoms bonded to carbon atoms were included in calculated positions and treated as riding atoms. The crystallographic data are summarized in Table 1. Selected bond lengths of the  $N,N$ -chelating ligand in **2–6** are listed in Table 2, where  $\text{C}_\alpha$ ,  $\text{C}_\beta$ , and  $\text{C}_\gamma$  are defined in Chart 2.

#### **DFT calculations**

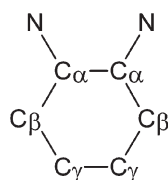
All DFT calculations were performed with B3LYP functionals<sup>52,53</sup> using the Gaussian 09 software package<sup>54</sup> and NBO<sup>55</sup> analysis was performed on the optimized structures. The 6-311G\*\* basis set was used for calculations of **3** and **4**. All geometry optimizations were performed starting from X-ray crystal structures. Both the 6-311G\*\* and 6-31G\* basis sets were used for the model complex simplified from compound **6** for spin density distribution. The coordinates of the model compound were derived from the crystal structure of **6** without geometry optimization.

Table 1 Crystallographic data

	2	3	4	5	6
Formula	C <sub>42</sub> H <sub>62</sub> Li <sub>2</sub> N <sub>2</sub> O <sub>3</sub>	C <sub>37</sub> H <sub>46</sub> FeN <sub>2</sub>	C <sub>33</sub> H <sub>38</sub> FeN <sub>2</sub> O <sub>3</sub>	C <sub>76</sub> H <sub>108</sub> Cl <sub>2</sub> Li <sub>2</sub> MoN <sub>4</sub> O <sub>4</sub>	C <sub>34</sub> H <sub>48</sub> LiN <sub>2</sub> O
FW	656.82	574.61	566.50	1494.81	507.68
T (K)	150(2)	150(2)	150(2)	150(2)	150(2)
Space group	P2 <sub>1</sub>	P2 <sub>1</sub> /n	P2 <sub>1</sub> /c	C2/c	P4 <sub>3</sub> ,2
a (Å)	10.9983(4)	10.5211(6)	16.3433(8)	21.8154(18)	10.4120(5)
b (Å)	17.1078(7)	17.3327(11)	11.3928(6)	25.039(3)	10.4120(5)
c (Å)	11.1127(4)	17.7438(17)	16.7688(8)	16.3773(13)	29.2952(15)
α (°)	90	90	90	90	90
β (°)	110.887(2)	91.243(4)	106.838(2)	118.185(4)	90
γ (°)	90	90	90	90	90
V (Å <sup>3</sup> )	1953.52(13)	3235.0(4)	2988.4(3)	7885.3(14)	3175.9(3)
Z	2	4	4	4	4
D <sub>c</sub> (g cm <sup>-3</sup> )	1.117	1.180	1.259	1.114	1.062
μ (mm <sup>-1</sup> )	0.068	0.493	0.539	0.280	0.062
No. reflns colld	11 742	28 548	60 497	23 017	28 934
No. indept reflns	3461	7423	9186	6890	2193
GOF on F <sup>2</sup>	1.027	1.020	1.005	1.061	1.016
R [I > 2σ(I)]	R <sub>1</sub> = 0.0296 wR <sub>2</sub> = 0.0779	R <sub>1</sub> = 0.0350 wR <sub>2</sub> = 0.0855	R <sub>1</sub> = 0.0570 wR <sub>2</sub> = 0.1111	R <sub>1</sub> = 0.0820 wR <sub>2</sub> = 0.1700	R <sub>1</sub> = 0.0587 wR <sub>2</sub> = 0.1633
R (all data)	R <sub>1</sub> = 0.0310 wR <sub>2</sub> = 0.0791	R <sub>1</sub> = 0.0493 wR <sub>2</sub> = 0.0927	R <sub>1</sub> = 0.1224 wR <sub>2</sub> = 0.1328	R <sub>1</sub> = 0.1277 wR <sub>2</sub> = 0.1829	R <sub>1</sub> = 0.0823 wR <sub>2</sub> = 0.1855

Table 2 Selected bond lengths (Å) of the chelating ligand

	2	3	4	5	6
C <sub>α</sub> –N	1.395(2) 1.396(2)	1.3663(19) 1.3605(19)	1.353(3) 1.354(3)	1.313(6) 1.310(6)	1.341(3)
C <sub>α</sub> –C <sub>α</sub>	1.439(2)	1.419(2)	1.425(3)	1.498(7)	1.478(5)
C <sub>α</sub> –C <sub>β</sub>	1.399(3) 1.394(3)	1.409(2) 1.413(2)	1.414(3) 1.414(3)	1.425(7) 1.428(6)	1.422(4)
C <sub>β</sub> –C <sub>γ</sub>	1.400(3) 1.397(3)	1.379(2) 1.374(2)	1.366(3) 1.369(3)	1.437(7) 1.444(7)	1.364(4)
C <sub>γ</sub> –C <sub>γ</sub>	1.384(3)	1.407(2)	1.417(4)	1.404(7)	1.400(6)

Chart 2 Labelling scheme of C<sub>α</sub>, C<sub>β</sub>, and C<sub>γ</sub>.

## Acknowledgements

We thank NSERC, the Canadian Foundation for Innovation and the Ontario Research Fund for funding. We also acknowledge Digital Specialty Chemicals for the gift of P<sup>t</sup>-Bu<sub>3</sub>.

## Notes and references

- 1 C. K. Jørgensen, *Coord. Chem. Rev.*, 1966, **1**, 164–178.
- 2 V. Lyaskovskyy and B. de Bruin, *ACS Catal.*, 2012, **2**, 270–279.
- 3 O. R. Luca and R. H. Crabtree, *Chem. Soc. Rev.*, 2013, **42**, 1440–1459.
- 4 A. L. Balch, F. Röhrscheid and R. H. Holm, *J. Am. Chem. Soc.*, 1965, 2301.
- 5 A. L. Balch and R. H. Holm, *J. Am. Chem. Soc.*, 1966, 5201.
- 6 L. F. Warren, *Inorg. Chem.*, 1977, **16**, 2814–2819.
- 7 A. B. P. Lever, H. Masui, R. A. Metcalfe, D. J. Stufkens, E. S. Dodsworth and P. R. Auburn, *Coord. Chem. Rev.*, 1993, **125**, 317–331.
- 8 A. B. P. Lever and S. I. Gorelsky, *Coord. Chem. Rev.*, 2000, **208**, 153–167.
- 9 A. B. P. Lever, *Coord. Chem. Rev.*, 2010, **254**, 1397–1405.
- 10 M. Kapovsky, C. Dares, E. S. Dodsworth, R. A. Begum, V. Raco and A. B. P. Lever, *Inorg. Chem.*, 2013, **52**, 169–181.
- 11 T. Matsumoto, H. Chang, M. Wakizaka, S. Ueno, A. Kobayashi, A. Nakayama, T. Taketsugu and M. Kato, *J. Am. Chem. Soc.*, 2013, DOI: 10.1021/ja4025116.
- 12 I. G. Fomina, A. A. Sidorov, G. G. Aleksandrov, S. E. Nefedov, I. L. Eremenko and I. I. Moiseev, *J. Organomet. Chem.*, 2001, **636**, 157–163.
- 13 I. L. Eremenko, S. E. Nefedov, A. A. Sidorov, M. O. Ponina, P. V. Danilov, T. A. Stromnova, I. P. Stolarov, S. B. Katser, S. T. Orlova, M. N. Vargaftik, I. I. Moiseev and Y. A. Ustynyuk, *J. Organomet. Chem.*, 1998, **551**, 171–194.
- 14 I. G. Fomina, A. A. Sidorov, G. G. Aleksandrov, V. N. Ikorskii, V. M. Novotortsev, S. E. Nefedov and I. L. Eremenko, *Russ. Chem. Bull.*, 2002, **51**, 1581–1587.
- 15 D. Herebian, E. Bothe, F. Neese, T. Weyhermüller and K. Wieghardt, *J. Am. Chem. Soc.*, 2003, **125**, 9116–9128.
- 16 E. Bill, E. Bothe, P. Chaudhuri, K. Chłopek, D. Herebian, S. Kokatam, K. Ray, T. Weyhermüller, F. Neese and K. Wieghardt, *Chem.–Eur. J.*, 2005, **11**, 204–224.
- 17 K. Chłopek, E. Bill, T. Weyhermüller and K. Wieghardt, *Inorg. Chem.*, 2005, **44**, 7087–7098.



- 18 J. Koller and R. G. Bergman, *Chem. Commun.*, 2010, **46**, 4577–4579.
- 19 J. V. Dickschat, S. Urban, T. Pape, F. Glorius and F. E. Hahn, *Dalton Trans.*, 2010, **39**, 11519–11521.
- 20 M. M. Khusniyarov, K. Harms, O. Burghaus, J. Sundermeyer, B. Sarkar, W. Kaim, J. van Slageren, C. Duboc and J. Fiedler, *Dalton Trans.*, 2008, 1355.
- 21 M. M. Khusniyarov, T. Weyhermüller, E. Bill and K. Wieghardt, *J. Am. Chem. Soc.*, 2009, **131**, 1208–1221.
- 22 N. A. Ketterer, H. Fan, K. J. Blackmore, X. Yang, J. W. Ziller, M. Baik and A. F. Heyduk, *J. Am. Chem. Soc.*, 2008, **130**, 4364–4374.
- 23 M. M. Khusniyarov, E. Bill, T. Weyhermüller, E. Bothe, K. Harms, J. Sundermeyer and K. Wieghardt, *Chem.–Eur. J.*, 2008, **14**, 7608–7622.
- 24 K. Chłopek, E. Bothe, F. Neese, T. Weyhermüller and K. Wieghardt, *Inorg. Chem.*, 2006, **45**, 6298–6307.
- 25 G. Buncic, Z. Xiao, S. C. Drew, J. M. White, A. G. Wedd and P. S. Donnelly, *Chem. Commun.*, 2012, **48**, 2570–2572.
- 26 M. M. Khusniyarov, T. Weyhermüller, E. Bill and K. Wieghardt, *Angew. Chem., Int. Ed.*, 2008, **47**, 1228–1231.
- 27 T. Wenderski, K. M. Light, D. Ogrin, S. G. Bott and C. J. Harlan, *Tetrahedron Lett.*, 2004, **45**, 6851–6853.
- 28 Y. Segawa, Y. Suzuki, M. Yamashita and K. Nozaki, *J. Am. Chem. Soc.*, 2008, **130**, 16069–16079.
- 29 S. Daniele, C. Drost, B. Gehrhus, S. M. Hawkins, P. B. Hitchcock, M. F. Lappert, P. G. Merle and S. G. Bott, *J. Chem. Soc., Dalton Trans.*, 2001, 3179.
- 30 P. Le Floch, F. Knoch, F. Kremer, F. Mathey, J. Scholz, W. Scholz, K. H. Thiele and U. Zenneck, *Eur. J. Inorg. Chem.*, 1998, 119.
- 31 S. C. Bart, E. J. Hawrelak, E. Lobkovsky and P. J. Chirik, *Organometallics*, 2005, **24**, 5518–5527.
- 32 P. Chaudhuri, C. N. Verani, E. Bill, E. Bothe, T. Weyhermüller and K. Wieghardt, *J. Am. Chem. Soc.*, 2001, **123**, 2213–2223.
- 33 P. B. Hitchcock, M. F. Lappert and X. Wei, *Dalton Trans.*, 2006, 1181–1187.
- 34 G. van Koten and K. Vrieze, *Adv. Organomet. Chem.*, 1982, **21**, 153.
- 35 K. Aoyagi, P. K. Gantzel, K. Kalai and T. D. Tilley, *Organometallics*, 1996, **15**, 923–927.
- 36 A. Anillo, M. R. Díaz, S. García-Granda, R. Obeso-Rosete, A. Galindo, A. Ienco and C. Mealli, *Organometallics*, 2004, **23**, 471–481.
- 37 E. A. Ison, K. A. Abboud, I. Ghiviriga and J. M. Boncella, *Organometallics*, 2004, **23**, 929–931.
- 38 A. Sattler, G. Zhu and G. Parkin, *J. Am. Chem. Soc.*, 2009, **131**, 7828–7838.
- 39 M. Brookhart, K. Cox, F. G. Cloke, J. C. Green, M. L. H. Green, P. M. Hare, J. Bashkin, A. E. Derome and P. D. Grebenik, *J. Chem. Soc., Dalton Trans.*, 1985, 423–433.
- 40 H. Yasuda and A. Nakamura, *Angew. Chem., Int. Ed. Engl.*, 1987, **26**, 723–742.
- 41 R. H. Crabtree, in *The Organometallic Chemistry of the Transition Metals*, Wiley, Hoboken, New Jersey, 2009, 5th edn, pp. 122–152.
- 42 H. M. McConnell and D. B. Chesnut, *J. Chem. Phys.*, 1958, **28**, 107.
- 43 J. C. M. Henning, *J. Chem. Phys.*, 1966, **44**, 2139.
- 44 S. D. Ittel, A. D. English, C. A. Tolman and J. P. Jesson, *Inorg. Chim. Acta*, 1979, **33**, 101–106.
- 45 M. M. Olmstead, P. P. Power and S. C. Shoner, *Inorg. Chem.*, 1991, **30**, 2547–2551.
- 46 F. Stoffelbach, D. Saurens and R. Poli, *Eur. J. Inorg. Chem.*, 2001, 2699–2703.
- 47 D. B. Dell'Amico, F. Calderazzo, C. della Porta, A. Merigo, P. Biagini, G. Lugli and T. Wagner, *Inorg. Chim. Acta*, 1995, **240**, 1–3.
- 48 D. R. Duling, *J. Magn. Reson., Ser. B*, 1994, **104**, 105–110.
- 49 *Apex 2 Software Package*, Bruker AXS Inc., 2008.
- 50 G. M. Sheldrick, *Acta Crystallogr., Sect. A: Foundam. Crystallogr.*, 2008, **64**, 112.
- 51 A. L. Spek, *J. Appl. Crystallogr.*, 2003, **36**, 7.
- 52 C. Lee, W. Yang and R. G. Parr, *Phys. Rev. B: Condens. Matter*, 1988, **37**, 785–789.
- 53 A. D. Becke, *J. Chem. Phys.*, 1993, **98**, 5648–5652.
- 54 M. J. Frisch, G. W. Trucks, H. B. Schlegel, G. E. Scuseria, M. A. Robb, J. R. Cheeseman, G. Scalmani, V. Barone, B. Mennucci, G. A. Petersson, H. Nakatsuji, M. Caricato, X. Li, H. P. Hratchian, A. F. Izmaylov, J. Bloino, G. Zheng, J. L. Sonnenberg, M. Hada, M. Ehara, K. Toyota, R. Fukuda, J. Hasegawa, M. Ishida, T. Nakajima, Y. Honda, O. Kitao, H. Nakai, T. Vreven, J. A. Montgomery, Jr., J. E. Peralta, F. Ogliaro, M. Bearpark, J. J. Heyd, E. Brothers, K. N. Kudin, V. N. Staroverov, T. Keith, R. Kobayashi, J. Normand, K. Raghavachari, A. Rendell, J. C. Burant, S. S. Iyengar, J. Tomasi, M. Cossi, N. Rega, J. M. Millam, M. Klene, J. E. Knox, J. B. Cross, V. Bakken, C. Adamo, J. Jaramillo, R. Gomperts, R. E. Stratmann, O. Yazyev, A. J. Austin, R. Cammi, C. Pomelli, J. W. Ochterski, R. L. Martin, K. Morokuma, V. G. Zakrzewski, G. A. Voth, P. Salvador, J. J. Dannenberg, S. Dapprich, A. D. Daniels, O. Farkas, J. B. Foresman, J. V. Ortiz, J. Cioslowski and D. J. Fox, *GAUSSIAN 09 (Revision B. 01)*, Gaussian, Inc., Wallingford CT, 2010.
- 55 A. E. Reed, R. B. Weinstock and F. Weinhold, *J. Chem. Phys.*, 1985, **83**, 735–746.